Journal of Engineering Physics and Thermophysics, Vol. 79, No. 1, 2006

ON SIMULATION OF TRANSFER PROCESSES IN THE FREEBOARD REGION OF A STEAM-GENERATOR FURNACE WITH A CIRCULATING FLUIDIZED BED

B. B. Rokhman

UDC 532.529:662.62

A semiempirical, stationary, two-zone model of transfer processes in the freeboard region of a reactor with a circulating boiling layer has been constructed. The features of the aerodynamics, heat and mass transfer, and combustion of anthracite culm in the core and near-wall ring region of a flow in a KFS-0.2 pilot plant have been investigated in detail.

A coal of the type of anthracite culm, which is used at present at electric power stations, differs significantly in its characteristics from the standard fuel, for which the power equipment of steam power plants is designed. Such coal cannot be burned in existing pulverized-coal fired boilers if it is not supplied with a gas or a fuel oil which prevents the removal of liquid and gaseous fuels from the power plant, deteriorates the operating characteristics of boilers, and adversely affects the environmental conditions. To eliminate the above-indicated problems, it is necessary to develop more efficient methods of processing of high-ash coals. One of these methods is to burn coal in a circulating fluidized bed.

The main element of a plant with a circulating fluidized bed is a reactor (Fig. 1), the lower part of which is a fluidized bed and the upper part of which represents a freeboard region. An upflow of a gas suspension propagates in the central region of the freeboard region (core zone) and a dense downflow of particles, providing an inward circulating of the solid phase in the furnace, propagates in the peripheral region (ring zone). A two-phase flow coming out from the reactor enters a cyclone, where the gas is separated from the dispersed phase. Then the dispersed phase is recycled back, through a settling post, to the reactor.

The aerodynamics of the freeboard region is characterized by the fact that the dispersed phase in it has a high concentration, which substantially enhances the mean motion and chaotic motion of poly- and monodisperse coke-sol particles and, therefore, the collisions between them. The pulsating motion of particles generates an energy that substantially influences the mixing of the solid phase and, consequently, the aerodynamic structure of the two-phase flow in the axial and radial directions [1].

Since transfer processes arise in the freeboard region of the systems considered at relatively low temperatures (850–950^{o}C), the main parameters determining the design of these systems are the time of stay of particles in the active zone (flow core) and their concentration (reaction surface). These two hydrodynamic parameters differently influence the combustion of coke-sol particles. For example, an increase in the mean dispersed-phase concentration in the cross section of the freeboard region β leads to an increase in the dispersed-phase concentration in the active zone β_c. In this case, the flow rate of particles in the peripheral ring zone increases; these particles practically do not participate in the combustion because of the small concentration of oxygen. On the other hand, the cross section of the core, through which more than 75% of the gas flow passes (see below), decreases, which leads to an increase in the flow rate of the gas suspension and a decrease in the time of its stay in the reaction zone. Thus, the aerodynamic structure characteristic of a circulating fluidized bed substantially influences the combustion of a solid fuel.

The computational procedure proposed is based on the following main assumptions: 1) the process considered is stationary; 2) the gas mixture consists of oxygen, carbon dioxide, and nitrogen; 3) the stoichiometric reactions occurring proceed by the scheme of the heterogeneous reaction $C + O_2 = CO_2$; 4) the concentration of carbon in the solid phase is constant throughout the freeboard region; 5) the dispersed phase in the freeboard region consists of

Institute of Coal-Power Production, National Academy of Sciences of Ukraine, 19 Andreevskaya Str., Kiev, 04070, Ukraine. Translated from Inzhenerno-Fizicheskii Zhurnal, Vol. 79, No. 1, pp. 20–28, January–February, 2006. Original article submitted May 17, 2004; revision submitted December 30, 2004.

monodisperse spherical coke-sol particles of diameter δ_{fb}, which allows one to determine the exponential decay γ of an actual process and, consequently, the change in the flow rate and in the concentration of the solid phase along the height of the freeboard region with the use of a simple measuring technique (this cannot be done in the case where the polydispersion of a two-phase flow is taken into account because it is difficult to experimentally determine the indicated parameters for each fraction); 6) the convective heat exchange between the carrying medium in the ring zone and the surface of the core particles located at the core–ring interface is negligibly small; 7) the gas-phase mass transfer between the core of the flow and the near-wall region, caused by the turbulent diffusion, is not taken into account because the kinetic energy of the turbulent pulsations of the carrying medium is substantially dissipated on the freeboard-region particles present in high concentrations and is expanded for the heterogeneous reactions [1]. The gas flows are redistributed between the core and the ring zone as a result of the changes in the cross sections of the zones and in the concentrations of particles in them along the height of the freeboard region.

Basic Equations and Boundary Conditions. It was experimentally established [2–4] that the flow rate and concentration of particles in the core of a flow in the reactor considered decrease exponentially along the height of the freeboard region as a result of the migration of the dispersed phase from the central part of the reactor to the peripheral region:

$$B_c = B_{c1} \exp(-\gamma z_{fb}), \tag{1}$$

$$\beta_c = \beta_{c1} \exp(-a z_{fb}), \tag{2}$$

where $z_{fb} = z - H_b$, $H_b \le z \le H_r$. Starting from this condition, we write the continuity equation for the solid phase

$$\frac{dB_c}{dz} = -\frac{dB_d}{dz}, \tag{3}$$

where

$$B_j = 3600 u_j \beta_j f_j \rho_p \quad (j = d, c). \tag{4}$$

Taking into account (1) and integrating (3) with the boundary condition $B_{d3} = 0$, we obtain

$$B_d = B_{c1} \exp(-\gamma z_{fb}) \left\{ \exp[-\gamma (H_r - z)] - 1 \right\}. \tag{5}$$

On the other hand, from the material-balance equation for the dispersed phase, $\bar{\beta} f_r = \beta_c f_c + \beta_d f_d$, one can obtain a relation between the concentrations of particles and the cross sections of both zones:

$$\frac{\bar{\beta} - \beta_d}{\beta_c - \beta_d} = \frac{f_c}{f_r}, \quad f_r = f_c + f_d. \tag{6}$$

It was shown in [5] that the function $\bar{\beta}$ appearing in expression (6) can be approximated, in the range $H_b \le z \le H_r$, by the exponential dependence

$$\bar{\beta} = \bar{\beta}_1 \exp(-\gamma z_{fb}). \tag{7}$$

The exponential decay constant γ will be determined for the reactor of a KFS-0.2 pilot plant [6], shown in Fig. 1. For this purpose, it is necessary to experimentally determine the difference between the pressures in the adjacent reactor regions positioned between cross section Nos. 1 and 2 and cross section Nos. 2 and 3. On the basis of these data one can calculate the average concentration of the dispersed phase in the indicated regions:

$$\bar{\beta}_{i,i+1} = \frac{\Delta P_{i,i+1}}{g \rho_p \Delta z_{i,i+1}}, \quad \Delta z_{i,i+1} = z_{i+1} - z_i \quad (i = 1, 2), \tag{8}$$

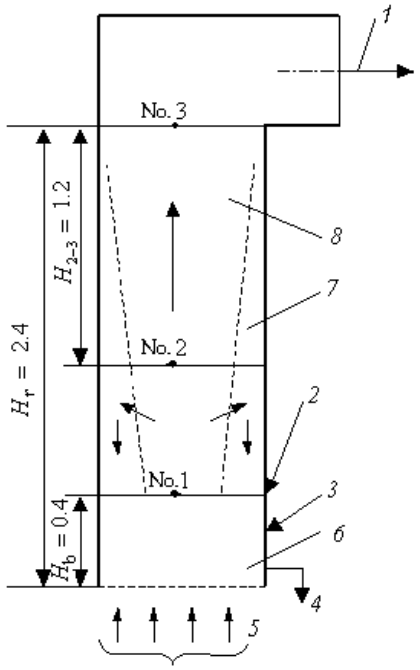

Fig. 1. Diagram of the reactor of a pilot KFS-0.2 plant: 1) gas-disperse-flow out; 2) initial-fuel feed; 3) recirculating-mass feed; 4) slag out; 5) feed of air to the region under the reactor lattice; 6) fluidized bed; 7) ring zone; 8) flow core; Nos. 1–3) cross sections.

and, using (7), the exponential decay γ along the height of the freeboard region

$$\gamma = -\frac{1}{\Delta z_{i+1/2,i+3/2}} \ln \frac{\bar{\beta}_{i+1,i+2}}{\bar{\beta}_{i,i+1}} \quad (i = 1) . \tag{9}$$

The continuity equation for the components of a gas mixture has, with allowance for the features of the aerodynamics of the freeboard region, the form

$$\frac{dG_j^{(1)}}{dz} = \frac{dW_j^{(1)}}{dz}, \quad \frac{dG_j^{(2)}}{dz} = -A_j + \frac{dW_j^{(2)}}{dz}, \quad \frac{dG_j^{(3)}}{dz} = \frac{11A_j}{8} + \frac{dW_j^{(3)}}{dz}, \tag{10}$$

where

$$A_j = \frac{6S_j^{(2)} k_j \beta_j G_j^{(2)} C_C}{(S_j^{(2)} + k_j)\, v_j \delta_{fb}}; \quad k_j = K \exp\left[-E/(T_j R)\right]; \quad \frac{dW_c^n}{dz} = -\frac{dW_d^n}{dz} \quad (n = 1, 2, 3) .$$

Summing the continuity equations for the components of the carrying medium (10) over all zones, we obtain the material balance equations for the gas in the core of the flow and the gas in the near-wall ring region:

$$\frac{dG_j}{dz} = \frac{3A_j}{8} + \frac{dW_j}{dz} . \tag{11}$$

The change in the total gas flow along the height of the freeboard region is determined from the equation

$$\frac{dG_r}{dz} = 3\,(A_d + A_c)/8 , \tag{12}$$

where

$$G_r = G_d + G_c\,; \quad G_j = 3600\rho_{gj} v_j f_j\,. \tag{13}$$

The right sides of Eqs. (10)–(12) account for the influence of the heterogeneous chemical reaction and the gas-phase mass transfer between the core and the near-wall region. The velocities of particles in each zone of the freeboard region are determined from the expression

$$v_j - u_j\,(1 - \beta_j) = \mathrm{Re}_j \nu_{gj}/\delta_{fb}\,, \tag{14}$$

where the Reynolds number is determined by the known Todes formula [7]

$$\mathrm{Re}_j = \frac{\mathrm{Ar}_j\,(1-\beta_j)^{4.75}}{18 + 0.61\sqrt{\mathrm{Ar}_j\,(1-\beta_j)^{4.75}}}\,, \quad \mathrm{Ar}_j = \frac{g\delta_{fb}^3\,(\rho_p - \rho_{gj})}{\nu_{gj}^2 \rho_{gj}}\,. \tag{15}$$

And finally, it is necessary to consider the heat state of the components of a two-phase flow. The energy equation for the solid phase has the form

$$\frac{d\,(c_j T_j B_j)}{dz} = \frac{A_j Q_h}{\mu^{(2)}} - 21\,600\,(\alpha_{radj} + \alpha_{convj})\,(T_j - \theta_j)\,\frac{\beta_j}{\delta_{fb}} f_j - \psi_j c_c T_c \left|\frac{dB_c}{dz}\right| - \psi_j q -$$

$$- 7200\varphi_j\,(\pi f_r)^{0.5}\,(\alpha_{rad,w} + \alpha_{cond,d})\,(T_d - t)\,, \tag{16}$$

$$q = 7200\,(\pi f_c)^{0.5}\,[\varepsilon_{red}\sigma\,(T_c^4 - T_d^4) + \varphi_j \alpha^*_{conv}\,(\theta_c - T_d)\,\beta_d/\beta_{max}]\,.$$

Here, j = c, d; $\psi_d = -1$; $\psi_c = 1$; $\varphi_d = 1$, $\varphi_c = 0$. The first term on the right side of Eq. (16) accounts for the heat released as a result of a heterogeneous chemical reaction, the second term accounts for the radiative and convective heat exchange between the gas and the particles, the third term accounts for the enthalpy transfer between the zones, the fourth term accounts for the radiative heat exchange between the zones and the convective heat exchange between the gas moving in the core of the flow and the surface of the ring-zone particles, located at the core–ring interface, and the last term accounts for the radiative and conductive heat exchange between the dense ring downflow and the wall.

The temperature of the gas is determined from the equation

$$\frac{d\,(h_j \theta_j G_j)}{dz} = h_m \theta_m \frac{dW_j}{dz} + 21\,600\,(\alpha_{radj} + \alpha_{convj})\,(T_j - \theta_j)\,\frac{\beta_j}{\delta_{fb}} f_j -$$

$$- 7200\,[\tau_j \alpha^*_{conv}\,(\theta_c - T_d)\,(\pi f_c)^{0.5}\,\beta_d/\beta_{max} + \varphi_j\,(\pi f_r)^{0.5}\,\alpha_{conv,w}\,(\theta_d - t)]\,, \tag{17}$$

where $\tau_d = 0$, $\tau_c = 1$; $\varphi_d = 1$, $\varphi_c = 0$; m = d, c ($m = j$ and $m \neq j$ if $dW_j/dz \geq 0$). The first term on the right side of Eq. (17) accounts for the gas-enthalpy transfer between the zones, the second term accounts for the heat exchange between the carrying medium and the dispersed phase, the third term accounts for the convective heat exchange between the gas moving in the core of the flow and the surface of the ring-zone particles located at the core–ring interface, and the last term accounts for the convective heat exchange between the gas found in the ring zone and the wall.

The density of the carrying medium and the pressure difference are determined from the expressions

$$\Delta P = g\rho_p \bar{\beta}_1\,[1 - \exp(-\gamma z_{fb})]/\gamma\,, \quad \rho_{gj} = 10^{-3} P/[R\theta_j\,(r_j^{(1)}/\mu^{(1)} + r_j^{(2)}/\mu^{(2)} + r_j^{(3)}/\mu^{(3)})]\,. \tag{18}$$

To close the system of equations obtained, it is necessary to formulate the boundary conditions at the upper (cross section No. 3) and lower (cross section No. 1) boundaries of the freeboard region (see Fig. 1).

Let us consider two variants. In variant A, the gas in the ring moves vertically up throughout the height of the freeboard region, and, in variant B, the gas moves in two directions. In the lower part of the freeboard region, the velocity of the gas at $H_b < z < z_x$ is negative, beginning with the cross section z_x ($v_d(z_x) = 0$). In the upper part of the freeboard region ($z_x < z > H_r$), the gas velocity is positive. At the input boundary of the freeboard region ($z = H_b$) the following parameters are determined: a) the density $\rho_{g,r1}$, the flow rate G_{r1}, and the mass fractions of the components r^n_{r1} of the gas mixture; b) the concentration of the dispersed phase in the ring zone β_{d1} and the gas pressure P_1; c) the diameter of the particles δ_{fb} and their density ρ_p; d) the concentration of carbon in the solid phase C_C and the temperature of the wall t.

The initial conditions for the temperatures of the phases (T_{j1}, θ_{j1}) and the rate flows of the gas components G^n_{j1} are determined depending on the calculation variant. For variant A,

$$G^n_{j1} = r^n_{r1} G_{j1}\,, \quad T_{c1} = \theta_{c1} = \theta_{d1}\,, \quad \rho_{gj1} = \rho_{g,r1}\,. \tag{19}$$

Moreover, the temperature T_{d1} is determined in advance, and the temperature T_{c1} is determined from the thermal balance equation for a fluidized bed

$$B_{fuel} c_{fuel} T_{fuel} + G_a h_a \theta_a + \Delta B_{b,C} Q_h / 12 + B_{c3} c_c \eta T_{c3} + B_{d1} c_d T_{d1} = G_{c1} h_c \theta_{c1} + G_{d1} h_d \theta_{d1} + B_{c1} c_c T_{c1} +$$

$$+ B_{slag} c_c T_{c1} + U\,. \tag{20}$$

For variant B:

$$G^n_{c1} = r^n_{r1} G_{r1} + \left| G^n_{d1} \right|\,, \quad G^n_{d1} = r^n_{d1} G_{d1}\,, \quad T_{c1} = \theta_{c1}\,.$$

The mass fractions of the gas components r^n_{d1} are determined on the assumption that all oxygen found in the ring zone near the surface of the fluidized bed burns up completely ($r^{(2)}_{d1} = 0$) because of the large concentration of particles ($\beta_{d1} = 0.2$–0.45) and the low velocity of the gas flow v_{d1}. For calculations, the values of T_{d1} and θ_{d1} are determined in advance and the temperatures of the phases in the core of the flow are calculated by (20). The density of the carrying medium ρ_{gj1} is determined from the equation of the gas state (18). The quantities determined in advance are then verified.

Since, at the output of the reactor, a two-phase flow moves vertically up at all points of the cross section of the channel, the following boundary conditions are set: $z = H_r$: $f_{c3} = f_r$, $\beta_{c3} = \beta_3$, $B_{d3} = 0$, $G_{d3} = 0$, $T_{d3} = T_{c3}$. The temperature of particles T_{c3} as well as the flow rate and density of the gas (G_{c^*}, ρ_{g,c^*}) in cross section No. 3 are determined in advance and are then verified in the process of calculations.

Computational Algorithm. In variant A, calculations are carried out in the following order:

1. The average concentrations of the dispersed phase β_1 and β_3 in the adjacent regions and the exponential decay constant γ are calculated by the differential pressures in these regions with the use of formulas (7)–(9).

2. The velocity of the gas v_{c3} at the output of the reactor is calculated from expression (13).

3. The velocity and flow rate of the particles (u_{c3}, B_{c3}) in cross section No. 3 is calculated by formulas (4), (14), and (15) and then the flow rates of the solid phase B_{c1} and B_{d1} at the input boundary of the above-layer space are calculated from expressions (1) and (5).

4. The system of equations (4), (6), (13)–(15) is solved for the nine unknowns β_{c1}, G_{j1}, u_{j1}, v_{j1}, and f_{j1} and the indicated parameters are determined at the input boundary of the freeboard region.

5. The exponential decay constant a is calculated by the known values of β_{c1} and β_{c3} from formula (2).

6. The flow rates of the gas components in the zones G^n_{j1} are calculated from expression (19) and the temperature T_{c1} is calculated by formula (20).

7. The system of differential equations (10)–(12), (16), (17) is approximated by finite-difference analogs. The equations are integrated by the Euler method with recalculation with a step selected depending on the number of iterations necessary for attainment of the required accuracy for each of the parameters.

TABLE 1. Initial Data for Calculation

Variant	ΔP_{1-2}, Pa	ΔP_{2-3}, Pa	β_{d1}	t, K	C_C
I	1406	792	0.3	1033	0.06
II	1406	792	0.25	1033	0.06
III	450	250	0.2	999	0.1
IV	450	250	0.3	999	0.12

8. The following iteration procedure is performed at each step of integration over the interval z, $z + \Delta z$: a) the initial temperature of the particles located everywhere over the height of the freeboard bed T_{dz} is assumed to be constant and equal to the initial temperature of the particles in the lower cross section of this bed; b) the indicated parameters in the cross section $z + \Delta z$ are calculated by the known values of B_{cz}, B_{dz}, β_z, and β_{cz} from expressions (1), (2), (5), and (7); the other unknown variables: $\omega_{z+\Delta z}\omega_z$ ($\omega = G_j^n$, G_j, G_r, T_c, θ_j, β_d, u_j, v_j, f_j, ρ_{gj}) are determined in the first iteration; c) the total gas-flow rate $G_{rz+\Delta z}$ is calculated by integrating Eq. (12); d) the parameters $\beta_{dz+\Delta z}$, $G_{jz+\Delta z}$, $u_{jz+\Delta z}$, $v_{jz+\Delta z}$, and $f_{jz+\Delta z}$ are determined by solving the system of algebraic equations (4), (6), (13)–(15); e) the value of $\Delta W_{jz,z+\Delta z}$ is determined by Eq. (11): $\Delta W_{jz,z+\Delta z} = G_{jz+\Delta z} - G_{jz} - 3A_{jz,z+\Delta z}\Delta z/8$; f) to calculate the variables $\Delta W^n_{jz,z+\Delta z}$, it is necessary to determine the direction of the gas motion, depending on the sign of the quantity $\Delta W_{jz,z+\Delta z}$, in the plane perpendicular to the z axis in the interval z, $z + \Delta z$: if gas moves from the core to the ring zone, the quantity $\Delta W_{cz,z+\Delta z}$ is negative and, consequently, $\Delta W^n_{cz,z+\Delta z} = -r^n_{cz,z+\Delta z}\left|\Delta W_{cz,z+\Delta z}\right|$ and $\Delta W^n_{dz,z+\Delta z} = -\Delta W^n_{cz,z+\Delta z}$ (see (10)); g) the unknowns $G^n_{jz+\Delta z}$, $T_{cz+\Delta z}$, and $\theta_{jz+\Delta z}$ are determined by solving differential equations (10), (16), and (17); h) the obtained values of the desired quantities are used as the initial parameters for the next iterations.

9. The parameters G_{c3} and $\rho_{g,c3}$, determined in the first iteration, are compared with the quantities G_{c^*} and ρ_{g,c^*} determined in advance; in the case where the quantities compared are different, the previous values of G_{c3} and $\rho_{g,c3}$ are changed for new ones and the calculation is repeated in the same order until the required accuracy is attained.

10. The difference in the temperature of particles located along the height of the freeboard region T_{dz} is calculated, beginning with the upper boundary of this region, using the earlier-determined quantities $G^{(2)}_{dz}$, θ_{jz}, β_{dz}, v_{dz}, f_{jz}, B_{jz}, T_{cz}, and $\rho_{g,dz}$ by Eq. (16). The calculated value of T_{d1} is compared to the previous value and, in the case where the values compared are different, a new value of T_{c1} is determined from (20) using a new value of T_{d1} and so on until the required accuracy is attained.

The computational scheme for variant B somewhat differs from the computational scheme for variant A. At the initial stage of calculation, the temperatures of the phases T_{dz} and θ_{dz} are assumed to be constant throughout the height of the freeboard region and equal to T_{d1} and θ_{d1}. Then, the cross section z_x is determined by solving the above-indicated system of equations. Equation (17) with boundary conditions $\theta_d(z_x) = \theta_c(z_x)$ is integrated with respect to the variables θ_{dz} over $H_b < z < z_x$ in the lower part of the freeboard region, by analogy with (16), from the top down and over $z_x < z < H_r$ in the upper part of the freeboard region from the bottom upwards.

Results of Calculations and Discussion. In accordance with the above-described algorithm, we have developed a program for calculating the aerodynamics, the heat and mass transfer, and the combustion of anthracite culm in the freeboard region of the furnace of a KFS-02 pilot plant of height H_r = 2.4 m and diameter D_r = 0.4 m at the following initial parameters: H_{1-2} = 0.8 m ($H_{1-2} = H_r - H_{2-3} - H_b$), H_{2-3} = 1.2 m, G_{r1} = 430 kg/h, $\delta_{fb} = 0.42\cdot10^{-3}$ m, ρ_p = 1800 kg/m^3, $r^{(1)}_{r1}$ = 0.73, $r^{(2)}_{r1}$ = 0.08, and $r^{(3)}_{r1}$ = 0.19. We now consider the results of calculation of the four variants, the initial conditions for which are presented in Table 1 (for variants I and IV, $r^{(1)}_{d1}$ = 0.71, $r^{(2)}_{d1}$ = 0, and $r^{(3)}_{d1}$ = 0.29).

Some results of calculation of the above-indicated processes are presented in Figs. 2–6. The cross-section area of the furnace is divided into two parts: the core of a flow and the near-wall ring zone (Fig. 1). The ratio between the areas of the zones positioned at the input to the freeboard region f_{d1}/f_{c1} changes depending on the initial concentrations of the dispersed phase β_1 and β_{d1} (Fig. 2, Table 1). Calculations have shown that the decrease in β_{d1} by 1.5 times at $\beta_1 = 4.74\cdot10^{-2}$ (Fig. 3, curves 3 and 4) increases the ratio f_{d1}/f_{c1} by 1.8 times (Fig. 2, curves 1 and 2), while the increase in the concentration β_1 from $4.74\cdot10^{-2}$ to 0.15 at β_{d1} = 0.25 increases this ratio by 10.3 times. In this case, the area of the core of the flow f_{c1II} accounts for 51.5% of the total area of the furnace (Fig. 2, curve 4). Note

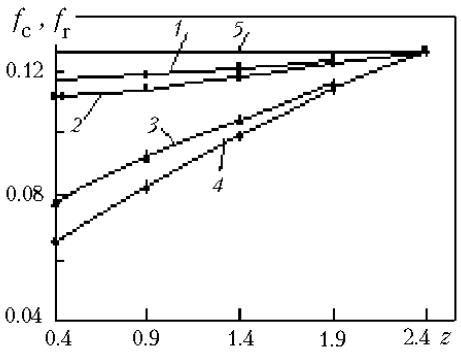

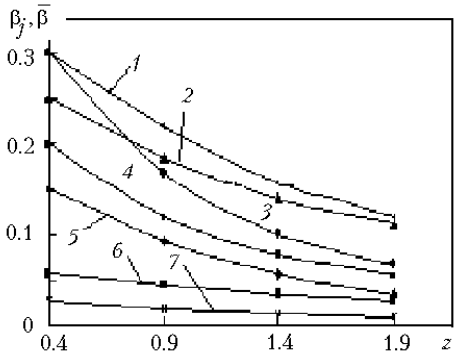

Fig. 2. Change in the cross section of the flow core along the height of the freeboard region above the fluidized bed: IV (1), III (2), I (3), and II (4); 5) f_r.

Fig. 3. Distribution of actual volume concentrations of particles: variant I: 1) β_d; variant II: 2) β_d, 5) β, 6) β_c; variant III: 4) β_d, 7) β_c; variant IV: 3) β_d.

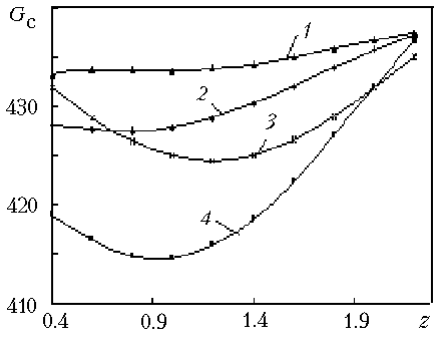

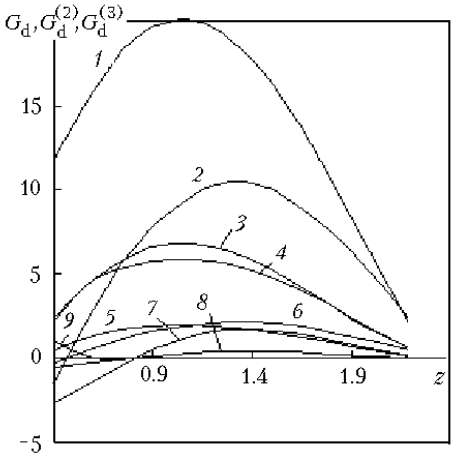

Fig. 4. Distribution of the gas-flow rates in the flow core along the height of the freeboard region above the fluidized bed: variants IV (1), III (2), I (3), and II (4).

Fig. 5. Distribution of the flow rates of the gas and its components in the ring zone: variant I: 2) G_d, 6) $G_d^{(3)}$; variant II: 1) G_d, 4) $G_d^{(3)}$, 9) $G_d^{(2)}$; variant III: 3) G_d, 5) $G_d^{(3)}$; variant IV: 7) G_d, 8) $G_d^{(3)}$.

that similar results ($f_{c1}/f_r = 0.45$) were obtained in experiments performed in [8] on a pilot plant with $H_r = 10$ m and $f_r = 0.071$ m^2 at the following initial data: $\rho_p = 1714$ kg/m^3, $\beta_{d1} = 0.25$, $v_r = 3.71$ m/sec, $\beta_1 \approx 0.16$, $\delta_{fb} = 0.076 \cdot 10^{-3}$ m, and $\theta_r = 298$ K. A narrowing of the input cross section of the flow core, caused by an increase in the quantity β_1 ($f_{c1III}/f_{c1II} = 1.72$ (Fig. 2, curves 2 and 4 are compared)) weakly influences the change in the flow rate of the carrying medium G_{c1} (Fig. 4, curves 2 and 4 are compared) but increases the velocity of the gas flow v_{c1} by 1.68 times and the velocity of particles u_{c1} by 3.4 times (Table 2, variants II and III are compared). In this case, the concentration of the dispersed phase in the active zone β_{c1} increases by two times (Fig. 3, curves 6 and 7 are compared), which undoubtedly influences the intensity of burn-out of the oxidizer in this region. We will analyze this circumstance in more detail by comparison of the rates of burn-out of oxygen in the core of the flow for variants II and III. It follows from Eq. (10) that the rate of burn-out of the oxidizer A_c is a function of the ratio β_c/v_c ($A_c = \chi(\beta_c/v_c)$). This relation, in turn, depends on the vertical coordinate $\beta_c/v_c = \xi(z)$. In variant III, the function $\xi_{III}(z)$ decreases at a much larger rate than the dependence $\xi_{II}(z)$. For example, the ratio ξ_{II}/ξ_{III} is equal to 1.2 at $z = 0.4$ m and 2.71 in the cross section $z = 1.9$ m. Such different behavior of the functions $\xi_{II}(z)$ and $\xi_{III}(z)$ is explained first of

TABLE 2. Some Results of Calculations

Quantities	z, m (variant II)				z, m (variant III)			
	0.4	0.9	1.4	1.9	0.4	0.9	1.4	1.9
v_d, m/sec	0.18	0.43	0.63	0.71	0.16	0.5	0.65	0.588
v_c, m/sec	5.98	4.61	3.89	3.46	3.55	3.5	3.38	3.3
u_d, m/sec	–0.84	–0.89	–0.96	–1.1	–1.13	–1.24	–1.39	–1.62
u_c, m/sec	4.1	2.5	1.63	1.11	1.2	1.03	0.88	0.74
$G_c^{(2)}$, kg/h	33.5	25.6	19.71	15.5	34.2	24.9	19.6	16.4

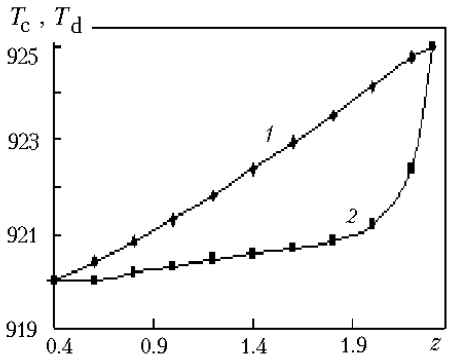

Fig. 6. Distribution of the temperatures T_j in the central and ring zones for variant II: 1) T_c; 2) T_d. T_j, °C.

all by the fact that the functions $\beta_c(z)$ and $v_c(z)$ in variant II decrease practically synchronously (Fig. 3, curve 6; Table 2, variant II), unlike variant III, where $v_c(z)$ changes weakly along the height of the freeboard region, as compared to $\beta_c(z)$, (Fig. 3, curve 7; Table 2, variant III). Thus, the rate of burn-out of oxygen in variant II is higher than that in variant III. Therefore, the concentration of carbon in the dispersed phase in variant III is higher than that in variant II (Table 1) at practically equal amounts of the oxidizer expended for the combustion in the freeboard region (Table 2).

Figure 5 shows the pattern of a gas flow in the ring zone. It is seen that, in the region of $0.4 < z < 1.4$ m, the function $G_d(z)$ increases monotonically as a result of the movement of gas from the core to the ring zone, which is evidenced by the decrease in the function $G_c(z)$ in this region (Fig. 4). At $z > 1.4$ m, the pattern changes. This is caused, first of all, by the change in the direction of the gas motion in the plane perpendicular to the z axis and by the decrease in the cross section of the ring zone. In variants I and IV (curves 2 and 7), in the region of $0.4 < z < 0.9$ m there arises a downflow because the concentrations of the dispersed phase in the ring zone in these variants are larger than in the other variants (Fig. 3, curves 1 and 2 and curves 3 and 4 are compared).

As was noted above, the ring zone practically does not participate in the combustion because of the small flow rate of the oxidizer (Fig. 5, curve 9). In the process considered, the ring zone serves as a screen that protects the reaction zone from the action of the cold wall, which is clearly seen from Fig. 6. Near the upper boundary of the above-layer space, where the temperatures T_c and T_d are close and the heat exchange between the zones is small, the function $T_d(z)$ sharply decreases with decrease in the coordinate, z changing in the range $1.9 < z < 2$ m, due to the heat exchange between the dense ring downflow and the wall (Fig. 6, curve 2). In the region of $z < 1.9$ m, the heat exchange between the zones is equilibrated by the heat flow directed to the wall of the reactor and, therefore, $T_d(z)$ changes weakly. Unlike the curve $T_d(z)$, the function $T_c(z)$ monotonically increases throughout the height of the freeboard region, which is explained by the predominance of the thermal effects of chemical reactions over the heat removal (Fig. 6, curve 1).

Thus, the semiempirical model, constructed by us, of the aerodynamics of the operating process and the heat and mass transfer in the freeboard region of a boiler allows one to determine the operating parameters of this boiler at different loads and optimize the combustion of a fuel. The computational procedure proposed can be used for calculating and verifying the design of such a boiler at the stages of detail and contractor design.

NOTATION

Ar, Archimedes criterion; a, γ, exponential decay constants, 1/m; B, flow rate of particles, kg/h; C, concentration; c, heat capacity of particles, kJ/(kg·K); D, diameter, m; E, activation energy, kJ/kmole; f, cross section, m^2; G, gas-flow rate, kg/h; g, free-fall acceleration, m/sec^2; h, heat capacity of gas, kJ/(kg·K); H, height, m; K, pre-exponential factor, m/sec; k, rate constant of a reaction, m/sec; P, gas pressure, N/m^2; Q, thermal effect of a reaction, kJ/kmole; q, heat exchange between zones, kJ/(h·m); R, universal gas constant, kJ/(kmole·K); Re, Reynolds number; r, mass fraction of a gas-mixture component; S, mass-transfer coefficient, m/sec; T, temperature of a particle, K (formulas) and ^oC (figures); t, temperature of the wall, K; U, heat flow to the wall, kJ/h; u, velocity of a particle, m/sec; v, total velocity of the gas in the streamwise section, m/sec; W, gas mass transferred between the core and the near-wall zone, kg/h; z, axial coordinate, m; α, heat-exchange coefficient, $kJ/(sec \cdot m^2 \cdot K)$; β, actual volume concentration of particles; δ, diameter of a particle, m; ε, degree of blackness; η, efficiency of a cyclone; θ, gas temperature, K; μ, molecular mass, kg/kmole; ν, kinematic viscosity, m^2/sec; ξ, χ, functions; ρ, density, kg/m^3; σ, Stefan–Boltzmann constant, $kJ/(sec \cdot m^2 \cdot K^4)$; ΔB, change in the mass of flow rate, kg/h; ΔP, differential pressure, N/m^2; Δz, integration step along the z axis, m. Subscripts: *, cross section No. 3; a, air; b, boiling layer; C, carbon; c, core of a flow; cond, conductive heat exchange; conv, convective heat exchange; d, dense downflow of particles in the ring zone; fb, freeboard region; fuel, initial fuel; g, gas; h, heat of a chemical reaction; i, number of cross section; j = d, c; m = d, c; max, maximum value; p, particle; r, reactor; rad, radiative heat exchange; red, reduced; slag, decanted ash (slag); w, wall; x, cross section of the ring zone in which the velocity of the gas flow is equal to zero; II, III, calculation variants. Superscripts: overscribed bar, averaged value; *, heat exchange between zones; n = 1, 2, 3; (1), nitrogen; (2), oxygen; (3), carbonic-acid gas.

REFERENCES

1. B. B. Rokhman and A. A. Shraiber, Mathematical modeling of the aerodynamics and physicochemical processes in the freeboard region above a circulating fluidized bed furnace. 1. Statement of the problem. Basic aerodynamic equations, *Inzh.-Fiz. Zh.*, **65**, No. 5, 521–526 (1993); 2. Interaction of particles (pseudoturbulence), *Inzh.-Fiz. Zh.*, **66**, No. 2, 159–167 (1994); 3. Boundary conditions. Some numerical results, *Inzh.-Fiz. Zh.*, **66**, No. 6, 681–688 (1994); 4. Heat and mass transfer and combustion, *Inzh.-Fiz. Zh.*, **67**, No. 1–2, 32–38 (1994).
2. E. U. Hartge, D. Rensner, and J. Werther, Solids concentration and velocity patterns in circulating fluidized beds, in: *Proc. 2nd Int. Conf.* "*Circulating Fluidized Bed Technology*," Pergamon, Oxford (1988), pp. 165–180.
3. L. W. Bolton and J. F. Davidson, Recirculation of particles in fast fluidized risers, in: *Proc. 2nd Int. Conf.* "*Circulating Fluidized Bed Technology*," Pergamon, Oxford (1988), pp. 39–42.
4. B. Hoggen, T. Lindstad, and T. A. Engh, Distribution of particles in the freeboard region above a fluidized bed, *Fluidization*, Eng. Found. Publ., New York (1986), pp. 297–304.
5. W. K. Lewis, F. D. Gilliland, and P. M. Lang, Entrainment from fluidized beds, *Chem. Eng. Progr. Symp. Ser.*, **58**, No. 38, 65–78 (1962).
6. A. Yu. Maistrenko, N. V. Chernyavskii, S. V. Yatskevich, and P. Gumel', Experimental combustion of a mixture of anthracite slime and culm in a circulating fluidized beds in laboratory plants of the Scientific-Technical Center of Coal Electrotechnologies, *Énergetika Elektrifikatsiya*, No. 6, 28–34 (1996).
7. A. P. Baskakov, B. P. Lukachevskii, I. P. Mukhlenov, et al., Design of Apparatuses with a Fluidized Bed. Handbook [in Russian], Khimiya, Leningrad (1986).
8. R. Bader, J. Findlay, and T. M. Knowlton, Gas/solids flow patterns in a 30.5-cm-diameter circulating fluidized bed, in: *Proc. 2nd Int. Conf.* "*Circulating Fluidized Bed Technology*," Pergamon, Oxford (1988), pp. 123–137.